Glacier changes in the Pascua-Lama region, Chilean Andes (29° S): recent mass balance and 50 yr surface area variations

A. Rabatel, H. Castebrunet, V. Favier, L. Nicholson, C. Kinnard

The Cryosphere, 5, 1029–1041, 2011
www.the-cryosphere.net/5/1029/2011/
doi:10.5194/tc-5-1029-2011

The Cryosphere

Glacier changes in the Pascua-Lama region, Chilean Andes (29° S): recent mass balance and 50 yr surface area variations

A. Rabatel[1,*], H. Castebrunet[1,], V. Favier[2], L. Nicholson[1,***], and C. Kinnard[1]**

[1]Centro de Estudios Avanzados en Zonas Aridas (CEAZA), Consorcio ULS/UCN/INIA, Casilla 599 – Campus Andres Bello, Colina El Pino s/n. La Serena, Chile
[2]UJF-Grenoble 1 /CNRS, Laboratoire de Glaciologie et Géophysique de l'Environnement UMR 5183, Grenoble, 38041, France
[*]now at: UJF-Grenoble 1/CNRS, LGGE UMR 5183, Grenoble, 38041, France
[**]now at: CEN, CNRM-GAME, Météo-France/CNRS, Saint Martin d'Hères, France
[***]now at: Institut für Geographie, Universität Innsbruck, Innsbruck, Austria

Received: 30 August 2010 – Published in The Cryosphere Discuss.: 2 November 2010
Revised: 4 November 2011 – Accepted: 6 November 2011 – Published: 22 November 2011

Abstract. Since 2003, a monitoring program has been conducted on several glaciers and glacierets in the Pascua-Lama region of the Chilean Andes (29° S/70° W; 5000 m a.s.l.), permitting the study of glaciological processes on ice bodies in a subtropical, arid, high-elevation area where no measurements were previously available. In this paper we present: (1) six years of glaciological surface mass balance measurements from four ice bodies in the area, including a discussion of the nature of the studied glaciers and glacierets and characterization of the importance of winter mass balance to annual mass balance variability; and (2) changes in surface area of twenty ice bodies in the region since 1955, reconstructed from aerial photographs and satellite images, which shows that the total glaciated surface area reduced by ∼29 % between 1955 and 2007, and that the rate of surface area shrinkage increased in the late 20th century. Based on these datasets we present a first interpretation of glacier changes in relation with climatic parameters at both local and regional scales.

1 Introduction

In the arid to semi-arid subtropical region of Chile and Argentina (27° S to 33° S), the evolution of the cryosphere (including glaciers, rock glaciers and seasonal snow cover) is a major concern for local populations due to the impact on water resources. Previous hydrological (e.g. Favier et al., 2009) and climatological (e.g. Masiokas et al., 2006; Vuille and Milana, 2007) studies carried out in this region highlight the lack of knowledge of glaciological processes at high elevation. The Pascua-Lama region (29°19′ S, 70°01′ W) is very close to the so-called "South America Arid Diagonal" (23–28°S, Schwerdtfeger, 1970); north from this area glaciers are scarce until the intertropical zone. Glaciers in Pascua-Lama region are generally small, and the term "glacieret" is often adapted. This term defines a very small ice body, typically less than 0.25 km^2 in extent, with no marked flow pattern visible at the surface, usually occupying sheltered parts of the landscape and formed primarily by drifting snow and avalanches (Cogley et al., 2011). The nearest monitoring sites to this subtropical region are Echaurren Glacier, Chile, 33°35′ S (Escobar et al., 2000), Piloto Glacier, Argentina, 32°27′ S (Leiva et al., 2007) to the south and Zongo and Chacaltaya glaciers ∼1500 km north in the Bolivian intertropical Andes, ∼16° S (e.g. Wagnon et al., 1999; Francou et al., 2003). Climate conditions are considerably drier in the Pascua-Lama region than those observed 450 km south on Echaurren Glacier or on the Argentinian side of the Andean divide on Piloto Glacier (Falvey and Garreaud, 2007; Favier et al., 2009). As a consequence, glaciological processes are likely to be different in this transition zone and studying the glaciers of this region is crucial to understand the role of glaciers in the hydrological cycle. Paleoglaciological studies (e.g. Kull et al., 2002; Ginot et al., 2006) have so far produced only limited knowledge of current local mass balance processes, patterns and relationship with local climatology. Previous work on glacier variations and relationship between

Correspondence to: A. Rabatel
((rabatel@lgge.obs.ujf-grenoble.fr)

glaciers and climate in this transition zone consists of four studies. In 1999, Leiva showed that the terminus of the Agua Negra Glacier in Argentina (30°10′ S, 69°50′ W) changed little from 1981 to 1997. Rivera et al. (2002) used aerial photographs to determine that Tronquitos Glacier (28°32′ S, 69°43′ W) retreated 0.52 km^2 over the 1955–1984 period which represents −11.4 % of its 1955 surface area. At Cerro Tapado summit (30°08′ S, 69°55′ W), Ginot et al. (2006) obtained a record of net accumulation over the 20th century from an ice core drilled down to the bedrock, which showed large interannual variability but no significant trend. Finally, Nicholson et al. (2009) showed in a recent inventory of the Huasco catchment (including the Pascua-Lama region) that the total glacierized area is very small (16.86 km^2). These studies need to be complemented in order to gain an understanding of glacier behaviour and its relation to present and future climate conditions.

Monitoring of several glaciers and glacierets in the Pascua-Lama region was initiated in 2003. This paper focuses first on the results of the glacier mass balance monitoring program in the Pascua-Lama region to understand the climate/glacier relationship within this subtropical zone. It then documents glacier changes over the last 50 yr. Finally, glacier changes over the last fifty years are discussed within the context of regional climate. The contribution of glacier ablation to the hydrological regime of the watershed is examined by Gascoin et al. (2011).

2 Study area

2.1 Pascua-Lama glaciers/glacierets

Figure 1 shows the studied ice bodies in the Pascua-Lama region located in the highest part of the Huasco River basin (southern part of the Chilean Región de Atacama). A small number of ice bodies are larger than 0.25 km^2 and show surface features indicative of ice flow and can be deemed glaciers, while other smaller bodies are more properly referred to as glacierets. Their distribution is mainly controlled by topography, with all ice bodies being found on the southern slopes of the highest summits, spanning a range of 4780–5485 m a.s.l (Nicholson et al., 2009). This distribution is a consequence of shading from solar radiation and the redistribution of snow by predominant northwesterly winds on the leeward sides of peaks and crestlines. All ice bodies have relatively smooth, gently sloping surfaces. Ice flow, where it exists, is minimal (2.0 ± 1.2 m a^{-1} on Guanaco Glacier for 2006, Golder Associates, 2009). Ice bodies surface areas range from 0.04 to 1.84 km^2 in 2007. Ground Penetrating Radar measurements made by Golder Associates (2009) on Guancaco, Estrecho and Ortigas 1 glaciers and Esperanza, Toro 1 and Toro 2 glacierets show that the ice is generally thin on the glacierets (<40 m) but can exceed 100 m on the glaciers (Table 1). All these ice bodies are most probably comprised of cold ice throughout and are thought to be cold-based; depth-averaged ice temperature measured in an ice core borehole drilled at 5161 m a.s.l. in the central part of Guanaco Glacier in November 2008 was −6.2 °C, and basal temperature at 112.5 m depth was −5.5 °C (Ginot, personal comunication, 2009).

2.2 Climatic conditions

Climate in northern Chile varies from extremely arid in the north (26° S) to Mediterranean in the south (33° S) (e.g. Falvey and Garreaud, 2007). The region is bounded by the Pacific Ocean to the West and by the Andes Cordillera to the East (reaching 6000 m a.s.l.), both of which exert an influence on climate conditions. Synoptic scale circulation is characterized by prevailing westerly winds, with a southward deflection of the flow along the Chilean side of the mountain range (Kalthoff et al., 2002). Annual average relative humidity remains below 40 % and clear skies predominate.

Precipitation shows a marked seasonality: 90 % occurs in winter between May and August (Fig. 2). Small precipitation events can occur at high elevation in the late summer (February and March) due to convective activity. The interannual variability of precipitation is mainly driven by the El Niño Southern Oscillation (ENSO), with warm phases (El Niño) associated with higher precipitation in this region of Chile, whereas a negative phase (La Niña) is associated precipitation deficits (Escobar and Aceituno, 1998). Quintana and Aceituno (2011) showed that during the 1950s, 1960s and 1970s, the frequency of humid years was abnormally low, but this changed into abnormally high frequency of humid years during the 1980s and the early 1990s, becoming low again during the late 1990s and early 2000s. Quintana and Aceituno (2011) mention that this sequence matches the most recent Pacific Decadal Oscillation (PDO) shifts that occurred in 1946 (change to negative phase), 1977 (change to positive phase), and 1998 (change to negative phase).

Automatic weather stations (AWS) operated within the Pascua-Lama mine site show the seasonality of temperature with warmer temperature during summer, i.e. December–January (Fig. 2). At "La Olla" station (3975 m a.s.l.) annual mean temperature is +1°C, while at "Frontera" station (4927 m a.s.l.), which coincides with the lower limit of glaciation, temperatures can be slightly positive for a few hours a day in summer, but monthly and annual mean temperatures remain negative year round (ranging between −0.6°C and −10.9°C for monthly means, and between −5.3°C and −6.8°C for annual means over the 2002–2008 period), so that precipitation at this elevation occurs mostly in solid form.

Climate variability over the 20th century has been characterized by decreasing precipitation (Santibañez, 1997; Quintana, 2004; Carrasco et al., 2005; Favier et al., 2009), and slightly increasing temperature (CONAMA, 2007). Causes

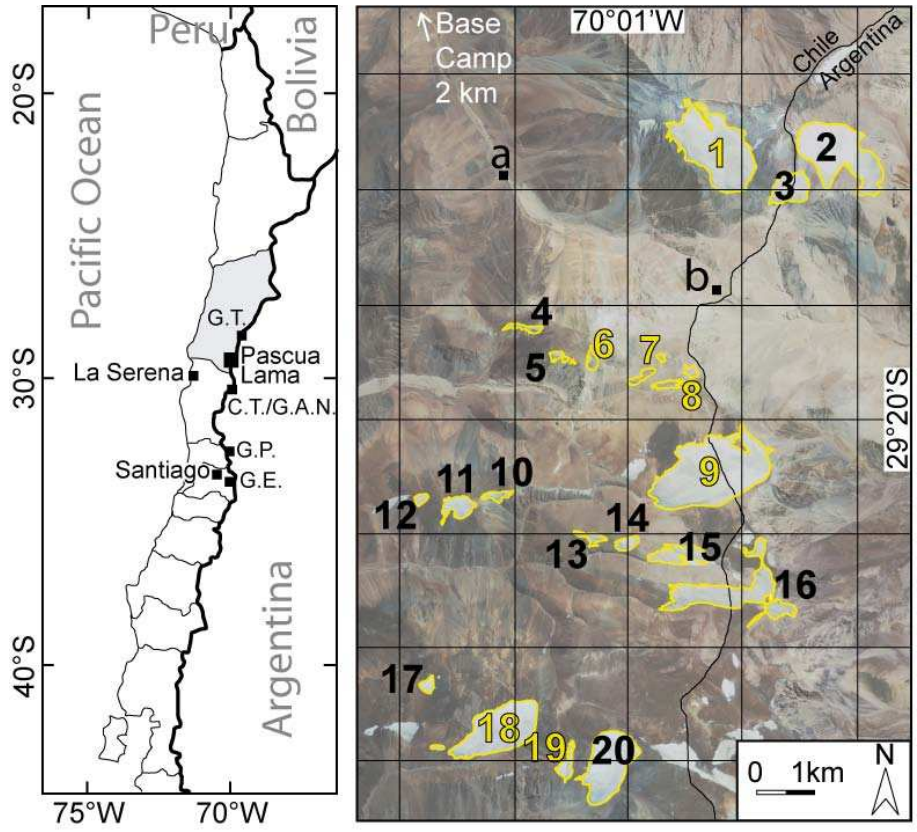

Fig. 1. Location of the Pascua-Lama region in the administrative Región de Atacama (in grey on the left map). On the left, the Northern and Central-south parts of Chile (G.T. = Glaciar Tronquitos; C.T. = Cerro Tapado; G.A.N. = Glaciar Agua Negra; G.P. = Glaciar Piloto; G.E. = Glaciar Echaurren). On the right, glaciers studied by CEAZA in the Pascua-Lama region are numbered in yellow: 1 = Estrecho; 6 = Esperanza; 7 = Toro 2; 8 = Toro 1; 9 = Guanaco; 18 = Ortigas 1; and 19 = Ortigas 2. For all the numbered glaciers, surface area change since the mid-20th century has been reconstructed (refer to Table 4). Black squares indicate "La Olla" **(a)** and "Frontera" **(b)** weather stations. Some glaciers of the area were not considered as they were not covered by the aerial photographs (for example north from glacier 2, east from glacier 20 or west from glacier 18). The background image is the 2005 Ikonos satellite image.

Table 1. Geographical and topographical characteristics of the monitored glaciers in the Pascua-Lama region (in 2007).

	Toro 1 Glacieret	Toro 2 Glacieret	Esperanza Glacieret	Guanaco Glacier	Estrecho Glacier	Ortigas 1 Glacier	Ortigas 2 Glacieret
Location	6 754 775 N	6,755 055 N	6 755 010 N	6 753 070 N	6 758 580 ,N	6,748 600 N	6 748 000 N
(UTM19S, WGS 84)	401 085 E	400 530 E	399 340 E	401 495 E	401 600 E	397 800 E	398 900 E
Surface area (km^2)	0.071	0.066	0.041	1.836	1.303	0.874	0.071
Max. elevation (m a.s.l.)	5235	5200	5145	5350	5485	5225	5245
Min. elevation (m a.s.l.)	5080	5025	4965	4985	5030	4775	4975
Max. thickness (m)[a]	20	12	36	120	–	–	–
Aspect	SSW	SSW	S	SSE	SE	SW	S
Number of ablation stakes[b]	(5) 9	(5) 5	4	(5) 14	(7) 14	(4) 9	1
First year of mass balance survey	2003	2003	2003	2003	2005	2005	2007

[a] 2004, _ means: no data are available
[b] in brackets = sites measured by Golder Associates S.A. (2003–2005), the other numbers represent the number of stakes measured by CEAZA.

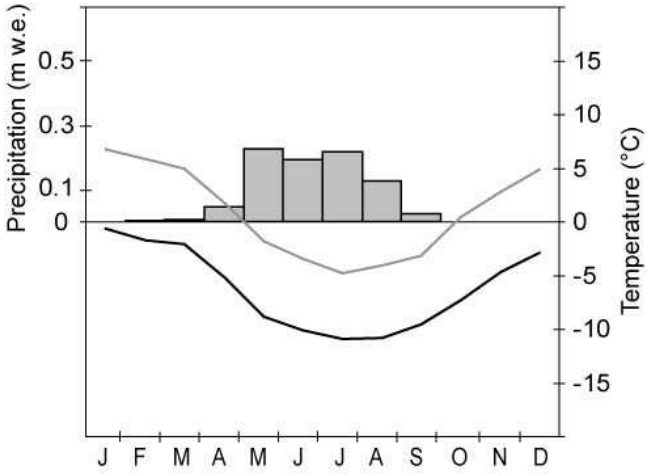

Fig. 2. Mean annual cycle (2001–2009) of monthly average precipitation (grey bars) and of monthly average temperature (lines) recorded in the Pascua-Lama area. Precipitation corresponds to manual measurements at Pascua-Lama Mine base camp Barriales (∼3800 m a.s.l.). Temperatures are recorded at "La Olla" (grey line; **(a)** on Fig. 1; 3975 m a.s.l.) and "Frontera" weather stations (black line; **(b)** on Fig. 1; 4927 m a.s.l.).

for reduced precipitation are not yet clearly understood, but in addition to ENSO/PDO variations (Escobar and Aceituno, 1998), high-latitude forcing from the Amundsen Sea region may provide an additional explanation for the observed secular drying trend by modulating the location of the winter storm tracks (Vuille and Milana, 2007).

3 Methods and data

Annual surface mass balance measurements using the glaciological method and floating-date system (Paterson, 1994) have been carried out since 2003 by Golder Associates S.A, and since 2007 by the glaciology group of the Centro de Estudios Avanzados en Zonas Aridas (CEAZA). Initially, three glacierets and one glacier were monitored (Esperanza, Toro 1, Toro 2 and Guanaco). Figure 3a, b show the distribution of the ablation stakes on these ice bodies. In 2005, two other glaciers (Estrecho and Ortigas 1) were added to the network and in 2007 a further glacieret (Ortigas 2) was added. The winter mass balance is calculated in early spring from: (1) snow depth and density measurements obtained by a combination of snow cores and probing at each stake site on the ice bodies; (2) stake emergence measurement; and (3) one or two snow pits are sampled on each glacier(et) depending on the size of the ice body. Summer mass balance is determined from elevation changes measured at bamboo stakes inserted in the ice (Fig. 3). For the areas where penitents can be found, several morphological parameters of the penitents are measured since 2007, such as: the size of the blade (length and width), the distance between two blades and the distance between the hollow and the foot of the stake (Fig. 4), giving more insight into the interpretation of mass balance measurements accuracy. The annual mass balance of the whole glacier, B_a, is calculated as:

$$B_a = \sum b_i \left(s_i / S\right) \text{ in m w.e.} \quad (1)$$

where b_i is the annual mass balance of an area i, for which surface area is denoted s_i, and S is the total ice body surface area. The ice body surface area was subdivided manually to allocate each stake a portion of glacier surface for which it was deemed representative. This surface area division was carried out primarily on the basis of elevation, with additional consideration of where transient snow cover, penitents or surface dust and debris were persistent surface features. This surface area division was kept constant for the study period.

Glacier surface topography was reconstructed using a digital elevation model (DEM) computed by the INFOSAT Company on the basis of a stereographic Ikonos satellite images pair acquired on 1 March 2005, so the DEM corresponds to conditions in the middle of the existing mass balance time series. Vertical and horizontal DEM precisions are ± 5 m on average.

Surface energy balance (SEB) measurements were also conducted by CEAZA with three AWS on Guanaco and Ortigas 1 glaciers and on the Toro 1 Glacieret (Fig. 3). The SEB will be presented in a forthcoming publication and will not be discussed here.

Glacier surface area was computed from aerial photographs taken by the Chilean Instituto Geografico Militar (IGM) and the Chilean Servicio Aerofotogrammétrico (SAF), and from Ikonos satellite images. The aerial photographs were taken on 27 April 1955 (IGM, scale = 1:70 000), 5 April 1956 (IGM, scale = 1:60 000), 31 May 1978 (SAF, scale = 1:60 000) and 26 November 1996 (SAF, scale = 1:50 000). Satellite images were acquired on 1 March 2005 and 26 March 2007 (1 m resolution). All images were geometrically corrected and georeferenced to the 2005 Ikonos image using the commercial PCI Geomatics® software. For each data source, a margin of uncertainty on the delineation of ice bodies was estimated. This results from: (1) the pixel size of the image or digital photograph; (2) the process of geometric correction; (3) the error associated with manual identification and delineation of the outline, which depends on the pixel size; and (4) a possible residual snow cover preventing the accurate visual identification of the edge of the glacier. Table 2 details the errors for each year and the resultant total uncertainty (root of the quadratic sum of the different independent errors). The uncertainty in the surface area is the total uncertainty on the delineation multiplied by the perimeter of the ice body (Perkal, 1956; Silverio and Jaquet, 2005).

Additional glaciological and climatological data sources used for the discussion of glacial changes over recent decades are given in Table 3.

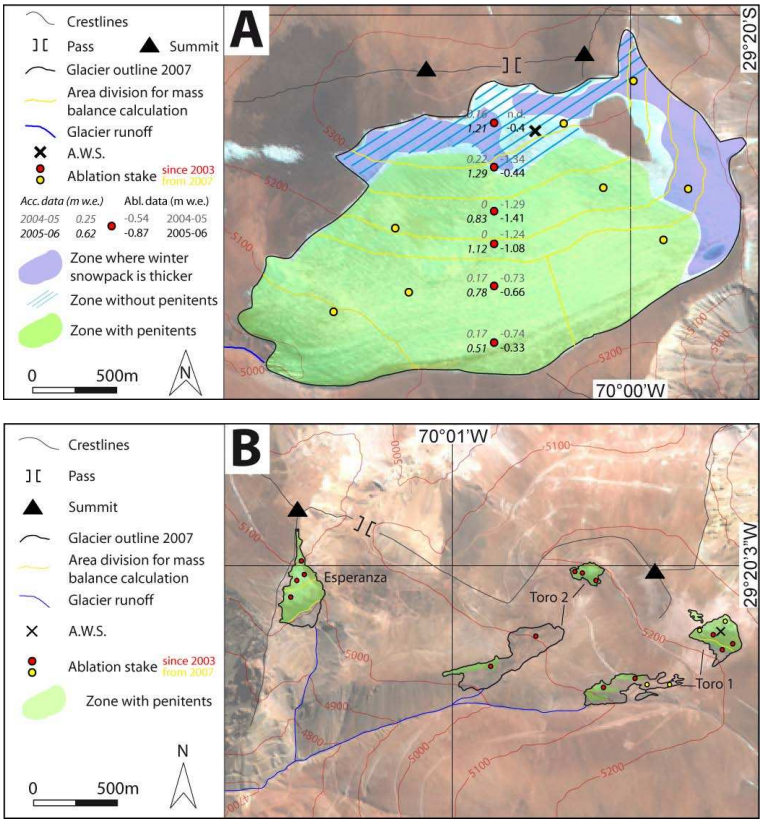

Fig. 3. **(A)** Guanaco Glacier with the location of the ablation stakes, the AWS and a qualitative delineation of area with/without penitents and area with a thicker winter snowpack. **(B)** Same representation for Esperanza, Toro 1 and 2 glacierets. Note that most of Toro 1 and 2 lower parts are debris-covered.

Table 2. Detail of errors associated with the images for each year. The largest error is related to the geometric correction. All images have been rectified on the basis of the 2005 Ikonos image, consequently the latter does not contain error due to this correction.

	Photo/Image source	Scale/Pixel size	Error due to the pixel size (m)	Error due to the geometric correction (m)	Error in the delineation (m)	Error due to a possible snow cover (m)	Total uncertainty (m)
1955	Hycon	1:70 000	1	20	3	10	23
1956	Hycon	1:60 000	4	14	4	0	15
1978	SAF	1:60 000	1	15	3	0	15
1996	SAF	1:50 000	2	8	4	0	9
2005	Ikonos	1 m	1	–	3	0	3
2007	Ikonos	1 m	1	7	3	0	8

4 Results and discussions

Firstly, we present and discuss results of the mass balance monitoring to characterize the climate-glacier relationship in semi-arid climate conditions. Only the three glacierets (Esperanza, Toro 1 and Toro 2) and Guanaco Glacier are considered, since they have the longest data series (six years). Secondly, glacier surface area changes since the mid-20th century are presented. Finally, we discuss possible causes of glacier changes over the last decades in light of the knowledge acquired through the current glacier mass balance monitoring, and other glaciological and climate data series.

4.1 Mass balance analysis

4.1.1 Accumulation and ablation processes at the glacier surface

The glaciological year in this region is from April to March. Accumulation occurs primarily during the winter season, i.e.

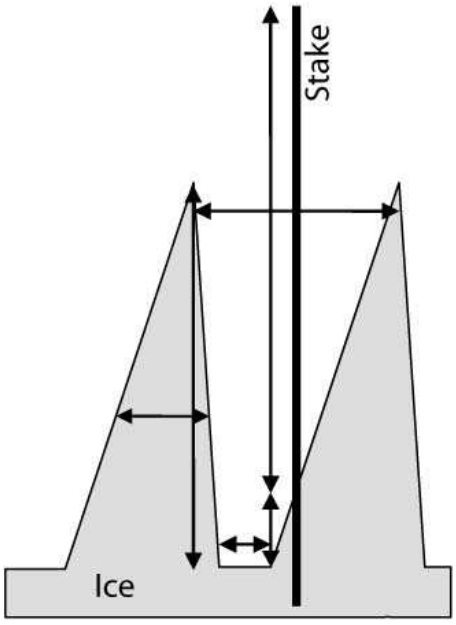

Fig. 4. Simplified scheme showing the measurements realised on the penitents themselves and the ablation stakes located in an area with penitents.

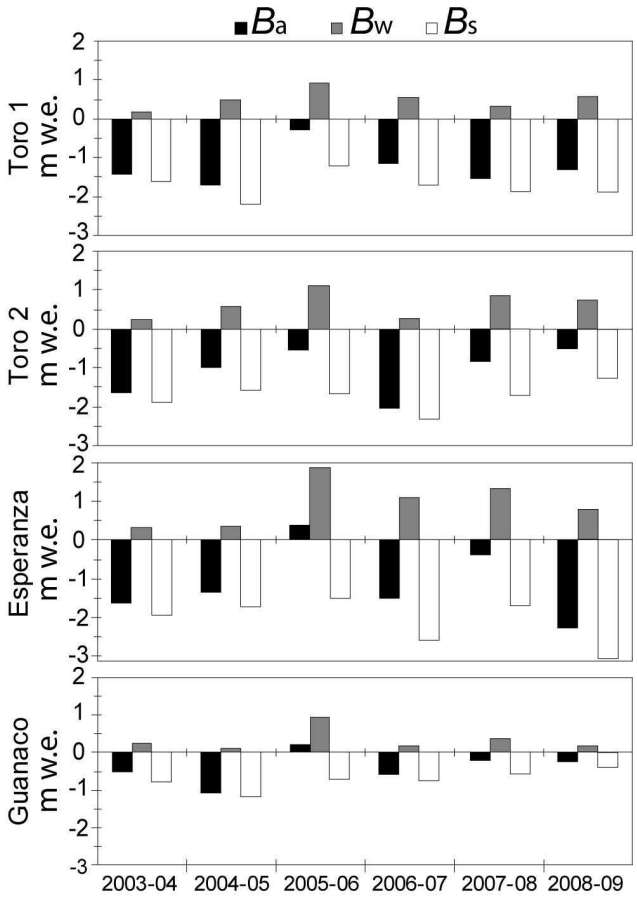

Fig. 5. Annual mass balance (B_a), winter mass balance (B_w) and summer mass balance (B_s) over the 2003–2009 period on Toro 1, Toro 2, Esperanza and Guanaco (in m w.e.)

April to September, whereas ablation dominates from October to March. Exceptionally dry or wet years can modify this simple scheme, and solid accumulation is possible at any time of year.

Ablation processes will be discussed in detail in a separate paper on the SEB data. We just mention here that: (1) ablation occurs by both melting and sublimation; and (2) summer snowfall events have a strong influence on ablation at the glacier surface by inhibiting melting (due to increased albedo), by limiting sublimation (due to decreased turbulence associated with reduction of the roughness length) and by isolating the body of the glacier from incident radiation and thus allowing a rapid decrease in ice temperature.

Accumulation results mainly from snow precipitation during winter. However, formation of superimposed ice was also observed during field campaigns over the spring and summer seasons. During the ablation season, surface temperature measured on Guanaco and Ortigas 1 glaciers drops below zero during the night (down to -20°C), so melt water from daytime melting refreezes during the night and superimposed ice is accreted to glacier ice and snow. The importance of this phenomenon in the distribution of mass balance over the ice bodies is hard to quantify and its estimation is beyond the focus of the current paper.

4.1.2 Annual mass balance and interannual variability

Figure 5 and Table 4 present the measured surface mass balance data for the four selected ice bodies in the Pascua-Lama region where six years of measurements are available. Over the six years, the average annual mass balance for the four ice bodies is -0.97 ± 0.70 m w.e. The glacierets (Toro 1, Toro 2 and Esperanza) show more negative annual mass balance values (-1.16 ± 0.68 m w.e.) than the biggest glacier of the area, Guanaco Glacier (-0.41 ± 0.43 m w.e.).

Over the 2003–2009 period, all ice bodies show large annual mass balance variability, which appears to increase with the glacier size (the coefficient of variation which measures the dispersion of a distribution, CV, is 73 % for the four ice bodies and 106 % for Guanaco Glacier). The mean summer mass balance measured on the four ice bodies is -1.58 ± 0.65 m w.e. (CV = 41 %) and the mean winter mass balance is 0.61 ± 0.44 m w.e. (CV = 72 %). Hence, the large winter mass balance variability has a dominant influence on the annual mass balance variability.

Within the study period, the 2005–2006 yr has the least negative annual mass balance (-0.05 ± 0.42 m w.e. on average for the four ice bodies). This quasi-balanced situation is linked to higher than normal precipitation (1.7 times higher than the 2001–2009 average recorded at Pascua-Lama base camp at 3800 m a.s.l.) associated with El Niño conditions,

Table 3. Additional data sources. Note that for NCEP/NCAR temperature reanalysis data, the period before 1958 was not considered because of large inhomogeneities.

Data	Source	Location	Duration
Annual mass balance	Chilean Dirección General de Aguas (Escobar, personal comunication, 2009)	Echaurren Glacier (33°35′ S, 70°08′W)	1975–2009
Niño 3 index	The International Research Institute for Climate and Society (http://iridl.ldeo.columbia.edu/SOURCES/.Indices/.nino/.EXTENDED/.NINO3/?help+datatables)	–	1955-2009
500 mbar temperature	NCEP/NCAR reanalysis (http://climexp.knmi.nl)	−31°25′; −28°75′ N 288°75′; 291°25′ E	1958–2007
Precipitation	Barrick Gold Corporation	El Indio Mine	1981–2005
Temperature		(29°51′ S, 70°02′ W, 3870 m)	1981–2002
Precipitation	Chilean Dirección General de Aguas	La Laguna dam (30°12′S, 70°02′W, 3130 m)	1965–2006

Table 4. Annual surface mass balance of the whole glacier, B_a; winter mass balace, B_w; and summer mass balance, B_s, for the 2003–2009 period of the studied ice bodies in the Pascua-Lama region (m w.e.).

Glacier		2003–2004	2004–2005	2005–2006	2006–2007	2007–2008	2008–2009
Toro 1	B_a	−1.43	−1.72	−0.28	−1.15	−1.55	−1.30
	B_w	0.19	0.47	0.92	0.56	0.34	0.60
	B_s	−1.62	−2.19	−1.20	−1.72	−1.89	−1.90
Toro 2	B_a	−1.65	−1.00	−0.53	−2.05	−0.85	−0.50
	B_w	0.23	0.58	1.11	0.26	0.87	0.77
	B_s	−1.88	−1.58	−1.64	−2.31	−1.72	−1.27
Esperanza	B_a	−1.64	−1.37	0.39	−1.50	−0.41	−2.29
	B_w	0.31	0.35	1.89	1.10	1.33	0.79
	B_s	−1.96	−1.72	−1.50	−2.60	−1.74	−3.09
Guanaco	B_a	−0.53	−1.07	0.21	−0.59	−0.21	−0.24
	B_w	0.25	0.11	0.93	0.17	0.36	0.16
	B_s	−0.78	−1.18	−0.72	−0.75	−0.57	−0.39

which are known to bring heavy snow accumulation (Escobar and Aceituno, 1998; Masiokas et al., 2006). In a general way, annual mass balance for the considered ice bodies is significantly correlated with precipitation recorded at Pascua-Lama base camp (for the four considered ice bodies: $0.63 < r < 0.93$, $p < 0.01$, $n = 6$).

4.1.3 Relationships between mass balance terms and altitude

Figures 6a, b and c respectively show the relationship between annual mass balance, winter mass balance and summer mass balance with altitude. On these figures, measurements made at each stake on the four ice bodies over the 2003–2008 period are all presented, but to improve clarity, each year has a different colour and measurements made on Guanaco Glacier are circled. It clearly appears that no relation exists between annual point mass balance and altitude. The concept of mass balance gradient is therefore meaningless for the ice bodies in this area.

Similarly, there is no relation between winter point mass balance and altitude (Fig. 6b). In fact, during wet years, i.e. El Niño years, the whole glacier remains covered by snow even at the end of the melt season and is therefore an accumulation area (e.g. J. Schmok, personal comunication, 2002–2003 yr). Conversely, for most years the glacier surface is predominantly snow free, or only patches of snow/firn remain at the end of the ablation season. These remaining snow/firn patches are in sheltered positions, where wind redistribution of snow generates a locally thicker winter snow pack, which is not related to the altitude but to the glacier topography. Consequently, concepts of accumulation/ablation zone and equilibrium-line altitude cannot be easily applied.

A weak, but not significant, negative correlation ($r^2 = 0.12$ with $p > 0.01$, $n = 109$, Fig. 6c) is found between summer point mass balance and altitude (ablation increasing with altitude) which may result from stronger melt at low elevation. Lower parts of the ice bodies may be more sheltered from high winds (high wind favours sublimation instead of melting, when sublimation consumes 8 times more energy than melting for ablation of the same w.e. mass of snow/ice), receive increased long wave radiation from surrounding valley sides, and experience longer time spent above freezing point at a daily time scale, all favouring melting during the ablation season. This hypothesis needs to be confirmed by SEB measurements.

4.1.4 Relationships between mass balance terms

Figure 7 shows the influence of summer mass balance and winter mass balance on the annual mass balance. The correlation coefficient between the six annual mass balance and winter mass balance pair values (summer mass balance) is $r = 0.75$ with $p < 0.01$ ($r = 0.76$ with $p < 0.01$) for the glacierets and $r = 0.80$ with $p < 0.01$ ($r = 0.71$ with $p < 0.01$) for Guanaco Glacier. This suggests that for the glacierets 56 % of the mass balance variability is produced by variations of winter mass balance and 58 % by summer mass balance, while for the glacier the corresponding percentages are 64 % and 51 %. Note that the sums exceed 100 % because winter mass balance and summer mass balance are not independent variables. The impact of winter mass balance

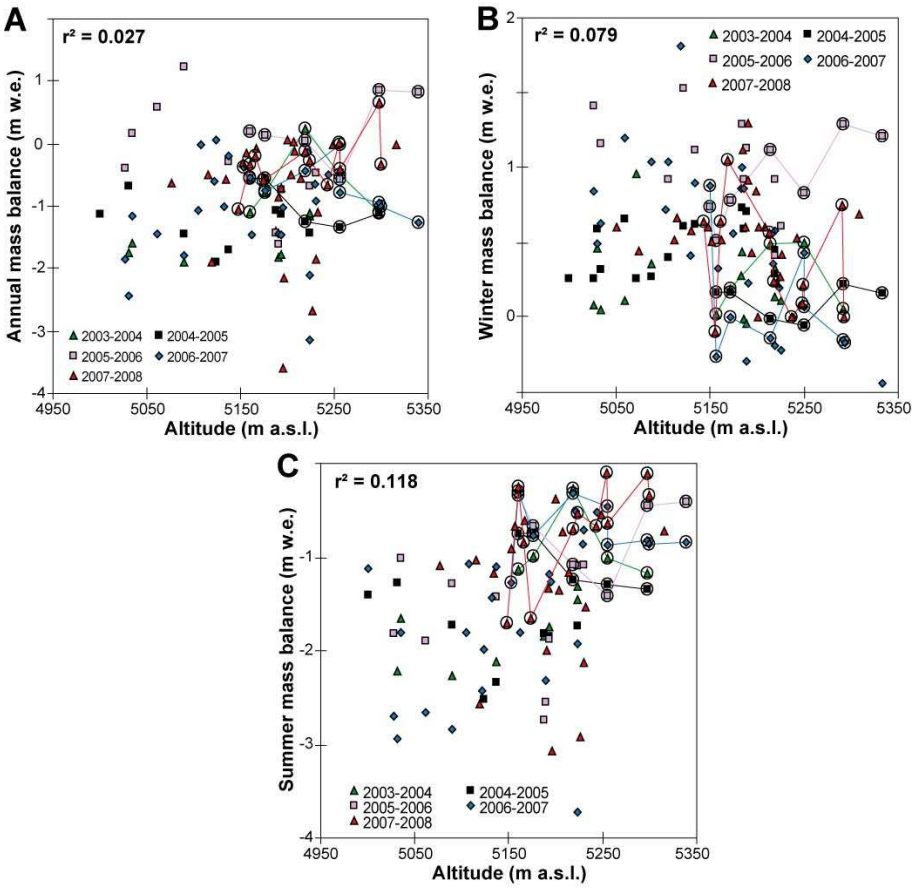

Fig. 6. (A) Comparison of annual mass balance measurements with altitude on Toro 1, Toro 2, Esperanza and Guanaco ice bodies over the 2003–2008 period. **(B)** Same comparison but with winter mass balance measurements. **(C)** Same comparison but with summer mass balance measurements. Lines and circles highlight measurements made on Guanaco Glacier for each year. r^2 values shown are for the linear best fit of stakes measured on all four ice bodies.

variability on annual mass balance variability appears to be stronger than for mid-latitudes glaciers where summer mass balance is the main control on interannual mass balance variations, e.g. in the French Alps, winter mass balance explains only 10–15 % of the annual mass balance variability (Vallon et al., 1998; Rabatel et al., 2008). This characteristic of Pascua-Lama ice bodies may result from both the higher variability of winter mass balance (72 %) and lower variability of summer mass balance (41 %) in this subtropical area compared to mid-latitudes. Similar conclusions can be drawn when comparing the results obtained on Pascua-Lama ice bodies with glaciers of the Arctic region where the variability of summer mass balance is the dominant factor in the annual mass balance variability (Koerner, 2005).

4.1.5 Causes of higher summer ablation on glacierets

Comparison of winter mass balance and summer mass balance between the glacierets and Guanaco Glacier shows that the more negative annual mass balance of the glacierets (Sect. 4.1.2) is mainly due to a more negative summer mass balance ($B_s = -1.86 \pm 0.46$ m w.e. for the glacierets and $B_s = -0.73 \pm 0.26$ m w.e. for Guanaco). This more negative summer mass balance might be partly attributable to the distribution of stakes on the glacierets, which extends to a lower elevation than on the glacier, but, as the altitude-dependence of ablation is very weak (Sect. 4.1.3; Figs. 3a, b and 6), and temperatures are persistently sub-zero at this elevation, the difference in summer balance between the ice bodies requires additional explanations. Possible causes of enhanced ablation on the glacierets are stronger edge effects, lower surface albedo due to natural dust and debris deposition, and penitents, which are all more evident on the glacierets than the glacier. Comparison of measured summer ablation and penitent height at 28 ablation stakes on the six ice bodies showed a significant correlation ($r^2 = 0.64$, $p < 0.01$, $n = 28$) between these variables. The observation of penitents on the glacierets is systematic in summer. Widespread surface dust deposits from the unglaciated surroundings may affect a larger portion of their surfaces, as they are small ice bodies, and favour penitent production.

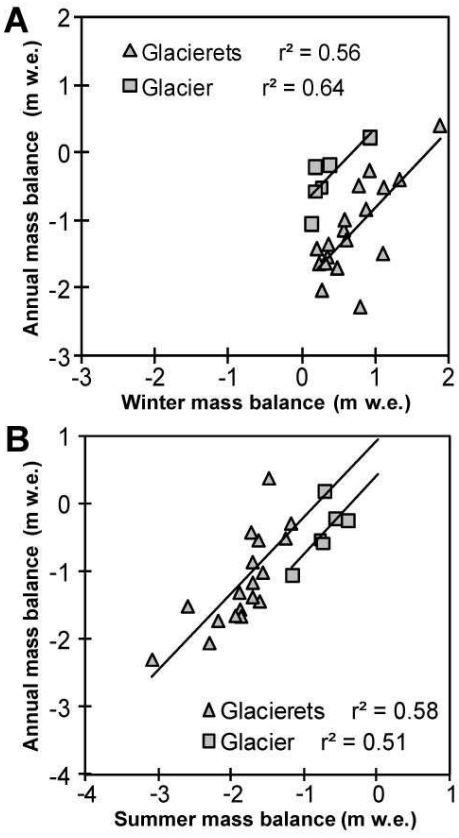

Fig. 7. **(A)** Comparison of annual mass balances and winter mass balances computed on Toro 1, Toro 2, Esperanza glacierets and Guanaco Glacier between 2003 and 2009. **(B)** Same comparison with summer mass balances. The background image is the 2007 Ikonos satellite image.

Indeed, laboratory measurements (Bergeron et al., 2006) have demonstrated that dust-covered snow forms penitents more readily, and has penitents with larger horizontal separations between the peaks than clean-snow surfaces. They also suggest that high intensity of radiation at thermal infrared wavelengths is crucial at the start of penitent growth; irradiance at these wavelengths is likely to be greater at the borders of the ice bodies due to a larger emission from surrounding rocks (e.g. Francou et al., 2003). Moreover, on the glacierets the development of large (meter scale) penitents is oberved. These are formed into the ice as well as snow, and thus persist into the subsequent year (Fig. 8). Unlike the glacierets, when penitents are observed on Guanaco Glacier, they are smaller (about a few tens of cm high) and some parts of the surface have no penitents. It is particularly the case at the level of the AWS (Figs. 3a, 8); where high wind (annual average of $6.4\,\mathrm{m\,s^{-1}}$ for Guanaco Glacier) prevents penitent formation; in agreement with results obtained by Bergeron et al. (2006).

The role of penitents has been discussed in several studies (e.g. Lliboutry, 1954; Corripio and Purves, 2005). Lliboutry (1954) mentions that melting is the main ablation process in a field of penitents. Thus, by creating and maintaining conditions more favourable to melting, the presence of penitents could partly explain the more negative summer mass balance on the glacierets.

Fig. 8. Photographs taken on 23 January 2008 (mid-summer) at the level of the AWS for Guanaco Glacier (left) and Toro 1 Glacieret (right), see Fig. 3a and b for location. While the surface of Guanaco Glacier does not have penitents, Toro 1 Glacieret is completly covered by penitents of snow (in the foreground) and of ice (in the vicinity of the AWS).

4.2 Glacier surface area changes

Surface area changes of six glaciers and fourteen glacierets in the Pascua-Lama region have been reconstructed from the mid-20th century using aerial photographs and satellite images (see Sect. 3). Results for each ice body are presented in Table 5, and Fig. 9 illustrates the contour change for Guanaco, Esperanza, Toro 1 and 2. Over the whole period, the total glaciated surface area reduced by about 29 % between 1955 and 2007. The loss is much larger for the glacierets (54 ± 16 %), than for the glaciers (19 ± 9 %), with a maximum of 79 % for Toro 2 Glacieret and a minimum of 9 % for Ortigas 1 Glacier.

The aerial photographs and satellite images used allow analysis of three periods of evolution: 1955/1956–1978 (23/22 yr), 1978–1996 (18 yr), and 1996–2007 (11 yr). Other aerial photographs exist, e.g. 1959 or 1981, but they do not cover the whole study area (for 1959) or were taken in spring (for 1981) when snow cover precludes the identification of glacier outlines. Figure 10 shows the annual surface area loss for each period, expressed as a percentage of the 1955/1956 surface area. The first period shows a mean annual surface area loss for all the ice bodies of $1.09 \pm 0.73\,\%\,\mathrm{a^{-1}}$ ($1.37 \pm 0.63\,\%\,\mathrm{a^{-1}}$ for the fourteen glacierets and $0.27 \pm 0.22\,\%\,\mathrm{a^{-1}}$ for the six glaciers). Over the second period, mean annual surface area loss falls to $0.47 \pm 0.46\,\%\,\mathrm{a^{-1}}$ ($0.56 \pm 0.49\,\%\,\mathrm{a^{-1}}$ for the fourteen glacierets and $0.18 \pm 0.14\,\%\,\mathrm{a^{-1}}$ for the six glaciers). During the last period, mean annual surface area loss for all the ice bodies increases to over twice the rate of the first period, at $2.34 \pm 1.32\,\%\,\mathrm{a^{-1}}$ ($2.74 \pm 1.20\,\%\,\mathrm{a^{-1}}$ for the fourteen glacierets and $0.96 \pm 0.61\,\%\,\mathrm{a^{-1}}$ for the six glaciers).

Table 5. Surface area change of twenty ice bodies in the Pascua-Lama region since the mid-20th century. Numbers of the first column refer to Fig. 1. Values in bold correspond to 1956.

N°	Local Name	Glacier surface area (km^2) 1955/1956	1978	1996	2005	2007	Loss between 1955/1956 and 2007
1	Estrecho	1.768	1.522	1.416	1.340	1.303	-26 ± 6 %
2	Los Amarillos	1.601	–	–	1.112	1.077	-33 ± 5 %
3	Amarillo	0.432	–	0.302	0.284	0.286	-34 ± 8 %
4		**0.134**	0.068	0.068	0.052	0.049	$-$**64** ± 9 %
5		**0.094**	0.046	0.044	0.039	0.038	$-$**60** ± 12 %
6	Esperanza	**0.186**	0.091	0.059	0.044	0.041	$-$**78** ± 5 %
7	Toro 2	**0.316**	0.185	0.166	0.070	0.066	$-$**79** ± 4 %
8	Toro 1	**0.257**	0.160	0.142	0.087	0.071	$-$**72** ± 6 %
9	Guanaco	2.170	2.002	1.935	1.849	1.836	-15 ± 4 %
10		**0.102**	0.078	0.076	0.060	0.053	$-$**48** ± 11 %
11		**0.267**	0.211	0.211	0.157	0.140	$-$**48** ± 8 %
12		**0.063**	0.049	0.046	0.033	0.030	$-$**53** ± 9 %
13		0.132	0.090	0.078	0.059	0.048	-63 ± 10 %
14		0.123	0.100	0.091	0.071	0.071	-42 ± 12 %
15		–	0.306	0.275	0.231	0.205	-33 ± 8 %*
16	Cañitos	–	1.045	1.039	0.878	0.810	-22 ± 9 %[a]
17		**0.069**	0.067	0.062	0.050	0.048	-30 ± 15 %
18	Ortigas 1	**0.963**	0.957	0.940	0.913	0.873	-9 ± 5 %
19	Ortigas 2	**0.165**	0.119	0.096	0.090	0.071	-57 ± 9 %
20		0.836	0.812	–	0.773	0.757	-9 ± 3 %

* loss between 1978 and 2007

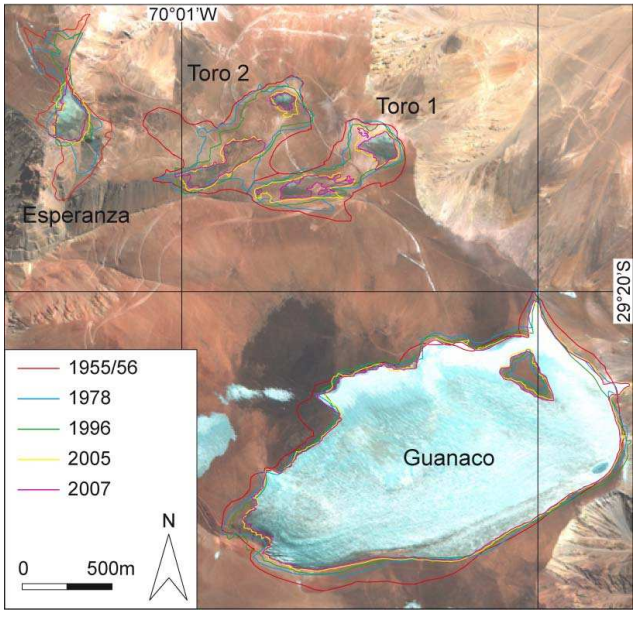

Fig. 9. Contour changes for Guanaco Glacier and Esperanza, Toro 1 and 2 glacierets over the 1955-2007 period.

Glacierets consistently experienced a greater percentage of surface area loss over all the periods than glaciers. In addition, the scatter between ice bodies is more pronounced with increasing mean surface area loss (Fig. 10), suggesting that topographic factors also influence the surface area changes.

4.3 Possible causes of glacier evolution since 1955

Figure 11 presents the mean surface area loss of all the studied ice bodies in parallel with glaciological and climatological data series. The Niño 3 index is an average of the sea surface temperatures in the region bounded by 90° W–150° W and 5° S–5° N. When the index is positive then waters are warmer than normal in the Niño 3 region, and conversely the index is negative when waters are cooler than normal in the Niño 3 region. El Niño (positive phase of the ENSO) occurs when the water in the Niño 3 region is much warmer than normal for a sustained period of time (e.g. Trenberth, 1997).

In Fig. 11, we present the cumulative annual mass balances of Echaurren Glacier between 1975 and 2009 and the Niño 3 index between 1955 and 2009. These data reveal an overall agreement between the Niño 3 index and mass balance variations. Actually, this link reflects the relationship between the annual mass balance at Echaurren Glacier and precipitation (Escobar et al., 2000). Although the period considered is short, annual mass balance series from Echaurren and Guanaco glaciers are significantly correlated ($r^2 = 0.75$, $p < 0.01$, $n = 7$). Note that this correlation analysis includes a highly positive annual mass balance for the year 2002–2003 estimated on Pascua-Lama ice bodies from GPR profile

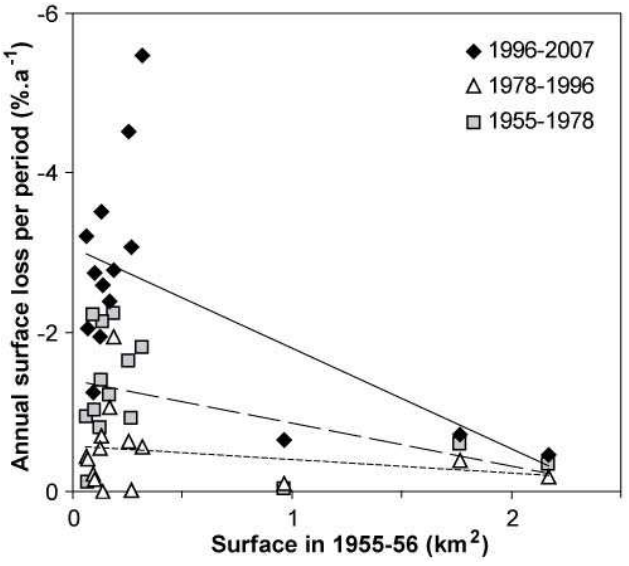

Fig. 10. Annual surface area loss per period for six glaciers and fourteen glacierets of the Pascua-Lama region in percent of their 1955–1956 surface area (see Table 5).Error bars are not shown for legibility of the graph; lines plotted are linear best fits for each period.

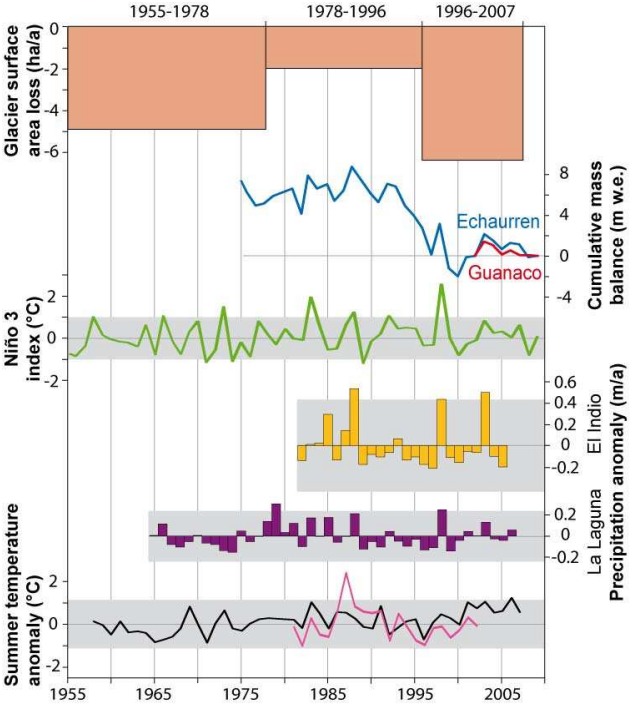

Fig. 11. Glacier surface area loss (average per period of all the studied ice bodies) compared with: (1) Echaurren (blue line) and Guanaco (red line) glaciers cumulative annual mass balance; (2) variation of the annual Nino3-SST (green line); (3) annual precipitation anomaly recorded at El Indio Mine and La Laguna dam; and (4) summer (NDJFM) temperature anomaly of NCEP/NCAR 500 mbar temperature reanalysis data (black line) and of El Indio Mine (pink line). Grey boxes for precipitation and temperature anomalies data represent the ± 2 standard deviation interval.

differencing (e.g. $B_a = 1.2$ m w.e. on Guanaco Glacier with an uncertainty of 15 %, J. Schmok, personal comunication, 2009). This method presents a lower accuracy to determine annual mass balance in comparison with the glaciological method, because of: (1) the uncertainties on the GPR measurements; and (2) the error resulting from the spatialisation at glacier scale of the measurements made on a few GPR profiles (2 or 3 per ice body). However, this estimated positive annual mass balance value on Guanaco Glacier is in good agreement with the highly positive annual mass balance measured using the glaciological method for the same year on Echaurren Glacier: $B_a = 2.06$ m w.e.

On a longer time scale, although limits of the periods considered for the glacier surface area changes are imposed by the available aerial photographs and satellite images, surface area changes of the small Pascua-Lama ice bodies show close agreement with the cumulative mass balance record of the larger Echaurren Glacier, located 450 km further south. The cumulative mass balance of Echaurren Glacier was quasi-stable between 1975 and 1993, in agreement with the low rate of surface area loss recorded on the Pascua-Lama ice bodies for the 1978–1996 period. Since the mid-1990s, Echaurren Glacier has shown generally negative mass balance values in agreement with more pronounced glacier surface area loss in the Pascua-Lama region.

Since precipitation is driven by the ENSO and represents a key factor at Echaurren Glacier (Escobar et al., 2000), we analysed precipitation variability in the study area. Figure 11 shows precipitation anomalies at two high-elevation sites located close to the Pascua-Lama region (El Indio Mine: 3870 m a.s.l., about 50 km south; La Laguna: 3130 m a.s.l., about 100 km south). Although longer time series would be advantageous for this analysis, during the positive ENSO years, both series present a positive precipitation anomaly. Mass balance time series at Pascua-Lama are too short for statistical comparison with precipitation records. However, despite the large distance between the sites, Echaurren Glacier mass balance is significantly correlated with La Laguna precipitation series ($r^2 = 0.62$, $p < 0.01$, $n = 31$) and El Indio precipitation series ($r^2 = 0.44$, $p < 0.01$, $n = 24$). These findings strengthen our hypothesis of a link between Pascua-Lama ice bodies changes and precipitation.

In contrast, no link between glacier mass balance and summer temperatures, nor between glacier surface area loss and temperature evolution over the last fifty years emerges. Considering annual mass balances and mean summer temperature for the November–March period (January–March period) at Frontera AWS (Fig. 1), the correlation coefficient and regression line slope are respectively 0.14 and 0.03 (0.37 and 0.19 respectively). Considering summer mass balances, the

same parameters for the same periods are respectively 0.31 and 0.14 (0.08 and 0.08 respectively), showing that correlation is not significant.

Figure 11 shows the summer (November to March) temperature anomaly at: (1) the 500 mbar pressure level (approximately the elevation of the ice bodies) for the Pascua-Lama region computed from NCEP/NCAR reanalysis data over the 1958–2007 period; and (2) El Indio Mine over the 1981–2002 period. For NCEP/NCAR 500 mbar temperature reanalysis data, both summer and annual averages present a slight positive trend (+0.19°C/decade for summer temperature over the 1958–2007 period), but not statistically significant if we consider the interannual variability. For El Indio Mine temperature data and considering that the period is shorter, the summer average presents no trend over the 1981–2002 period, whereas the annual average presents a slight but not statistically significant positive trend (+0.10°C/decade over the 1981–2002 period). The positive trend for annual average is in agreement with the results presented by Carrasco et al. (2005, 2008) and Falvey and Garreaud (2009) based on radiosonde stations and lowland meteorological stations. These studies show a cooling on the Chilean cost (at La Serena, 30° S) but a warming in the mountains and on the Argentinean piedmont at the same latitude.

Although the last decade shows the strongest mean annual surface area loss for all the studied ice bodies and more consistently positive temperature anomalies, we observed that the highest summer temperature anomalies in the NCEP/NCAR reanalysis data (2003 and 2006) are associated with the positive annual mass balances observed on Pascua-Lama ice bodies. Despite the lack of summer mass balance data for the year 2002–2003, the measured summer mass balance values suggest that ablation was reduced on the four ice bodies in 2005–2006. This is probably related to the fact that, as mentioned above, Pascua-Lama ice bodies are found at an altitude above the −5°C annual isotherm and thus melting is limited to few hours a day during the hottest summer periods. Hence, glacier surface area loss does not seem to be closely related to temperature evolution over the last fifty years.

All these considerations support the hypothesis that, in this region of the Andes, glacier surface area changes over the last decades have been primarily driven by the observed decreasing trend in precipitation (Santibañez, 1997; Quintana, 2004; Carrasco et al., 2005; CONAMA, 2007). The temperature changes observed during the last decades have had a secondary role.

5 Conclusions

Results from a new glacier mass balance monitoring program and the reconstruction of glacier surface area changes since the mid-20^{th} century on glaciers and glacierets in the subtropical Andes of Chile (29° S) have been presented in this study. This monitoring allows us to improve our knowledge and understanding of the behaviour of glaciers under semi-arid, high-elevation conditions (>5000 m a.s.l.).

1. Under such climatological and geographical conditions, where air temperature remains negative year round due to the high elevation, glacier annual mass balance is more strongly linked to variability in precipitation than air temperature.

2. The total glaciated surface area for the twenty studied ice bodies reduced by about 29 % between 1955 and 2007. After the first period, 1955–1978, the shrinkage rate slowed down between 1978 and 1996, and has accelerated since the late 1990s to reach a rate as high as experienced during the 1955–1978 period.

3. Although based on a short time-series, the mass balance record of Echaurren Glacier (33°35′ S) shows notable similarities to mass balance of Guanaco Glacier and surface area changes at Pascua-Lama despite the fact that the ice bodies are 450 km apart.

4. Glacier surface area changes in the Pascua-Lama region over the last decades result primarily from a decreasing trend in precipitation observed in the subtropical region over the last century. Because the ice bodies of the study area are located above the −5°C annual isotherm, and considering the lack of significant evidence for strong warming in this mountain region, we conclude that the temperature changes observed during the last decades have had a secondary role.

Acknowledgements. We thank R. Garrido, J. Marín, J. Araos, R. Ponce, J. L. Castro and E. Praderio (CEAZA) as well as all those who took part in field measurements. Project funding and logistical support in the Pascua-Lama area were provided by the Compañía Minera Nevada. We thank G. Casassa (handling editor), J. G. Cogley. M. Pelto, J. Carrasco and an anonymous referee for their constructive comments used to improve the paper.

Edited by: G. Casassa

References

Bergeron, V., Berger, C., and Betterton, M. D.: Controlled irradiative formation of penitents, Phys. Rev. Lett., 96, 098502, doi:10.1103/PhysRevLett.96.098502, 2006.

Carrasco, J. F., Casassa, G., and Quintana, J.: Changes of the 0°C isotherm in central Chile during the last Quarter of the 20th Century, Hydrol. Sci. J., 50, 933–948, 2005.

Carrasco, J. F., Osorio, R., and Casassa, G.: Secular trend of the equilibrium line altitude in the western side of the southern Andes derived from radiosonde and surface observations, J. Glaciol., 54, 538–550, 2008.

Cogley, J. G., Hock, R., Rasmussen, L. A., Arendt, A. A., Bauder, A., Braithwaite, R. J., Jansson, P., Kaser, G., Möller, M., Nicholson, L., and Zemp M.: Glossary of Glacier Mass Balance and Related Terms, IHP-VII Technical Documents in Hydrology No. 86, IACS Contribution No. 2, UNESCO-IHP, Paris, 2011.

CONAMA: Resultados Proyecto Estudio de la variabilidad Climática en Chile para el Siglo XXI, by DGF/UCH for CONAMA, CONAMA report, 2007.

Corripio, J. G. and Purves, R. S.: Surface energy balance of high altitude glaciers in the central Andes: the effect of snow penitentes, in: Climate and Hydrology in Mountain Areas, edited by: de Jong, C., Collins, D., and Ranzi, R., Wiley and Sons, London, 15–27, 2005.

Escobar, F. and Aceituno, P.: Influencia del fenómeno ENSO sobre la precipitación nival en el sector andino de Chile Central durante el invierno austral, Bull. Inst. Fr. Etudes Andines, 27, 753–759, 1998.

Escobar, F., Casassa, G., and Garín, C.: 25 yr record of mass balance of Echaurren glacier, central Chile, and its relation with ENSO events, in: Proceedings, Sixth International Conference on Southern Hemisphere Meteorology and Oceanography, Santiago de Chile, 3–7 April 2000, American Meteorological Society: Santiago de Chile; 118–119, 2000.

Falvey, M. and Garreaud, R.: Wintertime precipitation episodes in central Chile: associated meteorological conditions and orographic influences, J. Hydrometeorol., 8, 171–193, 2007.

Falvey, M. and Garreaud, R.: Regional cooling in a warming world: Recent temperature trends in the southeast Pacific and along the west coast of subtropical South América (1979–2006), J. Geophys. Res., 114, D04102, doi:10.1029/2008JD010519, 2009.

Favier, V., Falvey, M., Rabatel, A., Praderio, E., and López, D.: Interpreting discrepancies between discharge and precipitation in high-altitude area of Chile's Norte Chico region (26–32° S), Water Res., 45, W02424, doi:10.1029/2008WR006802, 2009.

Francou, B., Vuille, M., Wagnon, P., Mendoza, J., and Sicart, J. E.: Tropical climate change recorded by a glacier in the central Andes during the last decades of the twentieth century: Chacaltaya, Bolivia, 16° S, J. Geophys. Res., 108, doi:10.1029/2002JD002959, 2003.

Gascoin, S., Kinnard, C., Ponce, R., Lhermitte, S., MacDonell, S., and Rabatel, A.: Glacier contribution to streamflow in two headwaters of the Huasco River, Dry Andes of Chile, The Cryosphere Discuss., 4, 2373–2413, doi:10.5194/tcd-4-2373-2010, 2010.

Golder Associates S. A.: Área de Pascua Lama, Tercera Región de Atacama, Recopilación de estudios de línea base actualizada de la criósfera, Informe: 0792155016-3.0-IT 005, (info@golder.cl), 2009.

Ginot, P., Kull, C., Schotterer, U., Schwikowski, M., and Gaeggeler, H. W.: Glacier mass balance reconstruction by sublimation induced enrichment of chemical species on Cerro Tapado (Chilean Andes), Clim. Past, 2, 21–30, 2006, http://www.clim-past.net/2/21/2006/.

Kalthoff, N., Bischoff-Gauss, I., Fiebig-Wittmaack, M., Fiedler, F., Thürauf, J., Novoa, J.-E., Pizarro, C., Gallardo, L., and Rondanelli, R.: Mesoscale wind regime in Chile at 30° S, J. Appl. Meteorology, 41, 953–970, 2002.

Koerner, R. M.: Mass balance of glaciers in the Queen Elizabeth Islands, Nunavut, Canada, Ann. Glaciol., 42, 417–423, 2005.

Kull, C., Grosjean, M., and Veit, H.: Modelling modern and late Pleistocene glacio-climatological conditions in the north Chilean Andes (29–30° S), Clim. Change, 52, 359–381, 2002.

Leiva, J. C.: Recent fluctuations of the Argentinian glaciers, Global Planet. Change, 22, 169-177, doi:10.1016/S0921-8181(99)00034-X, 1999.

Leiva, J. C., Cabrera, G. A., and Lenzano, L. E.: 20 yr of mass balances on the Piloto glacier, Las Cuevas river basin, Mendoza, Argentina, Global Planet. Change, 59, 10–16, 2007.

Lliboutry, L.: The origin of penitents, J. Glaciolo., 2, 331–338, 1954.

Masiokas, M. H., Villalba, R., Luckman, B. H., Le Quesne, C., and Aravena, J. C.: Snowpack variations in the Central Andes of Argentina and Chile, 1951–2005: large-scale atmospheric influences and implications for water resources in the region, J. Clim., 19, 6334–6352, 2006.

Nicholson. L., Marín, J., Lopez, D., Rabatel, A., Bown, F., and Rivera, A.: Glacier inventory of the upper Huasco valley, Norte Chico, Chile: glacier characteristics, glacier change and comparison to central Chile, Ann. Glaciol., 50, 111–118, 2009.

Paterson, W. S. B.: The physics of glaciers, 3rd Edition, Butterworth-Heinemann Ltd, 496 pp., 1994.

Perkal, J.: On epsilon length, Bull. Acad. Pol. Sci., 4, 399–403, 1956.

Quintana, J.: Estudio de los factores que explican la variabilidad de la precipitación en Chile en escalas de tiempo interdecadal, MSc thesis, Universidad de Chile, 2004.

Quintana, J. and Aceituno, P.: Changes in the rainfall regime along the extratropical west coast of South America (Chile) during the 20th Century, J. Clim., submitted, 2011.

Rabatel, A., Dedieu, J.-P., Thibert, E., Letréguilly, A., and Vincent, C.: Twenty-five years (1981–2005) of equilibrium-line altitude and mass balance reconstruction on Glacier Blanc in the French Alps using remote sensing methods and meteorological data, J. Glaciol., 54, 307–314, 2008.

Rivera, A., Acuña, C., Casassa, G., and Bown, F.: Use of remote sensing and field data to estimate the contribution of Chilean glaciers to sea level rise, Ann. Glaciol., 34, 367–372, 2002.

Santibañez, F.: Tendencias seculares de la precipitación en Chile, in: Diagnóstico climático de la desertificación en Chile, edited by: Soto, G. and Ulloa, F., CONAF, La Serena, Chile, 1997.

Schwerdtfeger, W.: Climates of Central and South America, Vol. 12: World Survey of Climatology, New York, Elsevier, 1970.

Silverio, W. and Jaquet, J.-M.: Glacial cover mapping (1987–1996) of the Cordillera Blanca (Peru) using satellite imagery, Remote Sens. Environ., 95, 342–350, 2005.

Trenberth, K. E.: The definition of El Niño, B. Am. Meteorol. Soc., 78, 2771–2777, 1997.

Vallon, M., Vincent, C., and Reynaud, L.: Altitudinal gradient of mass balance sensitivity to climatic change from 18 yr of observations on Glacier d'Argentière, France, J. Glaciol., 44, 93–96, 1998.

Vuille, M. and Milana, J. P.: High-latitude forcing of regional aridification along the subtropical west coast of South America, Geophys. Res. Lett., 34, L23703, doi:10.1029/2007GL031899, 2007.

Wagnon, P., Ribstein, P., Francou, B., and Pouyaud, B.: Annual cycle of energy balance of Zongo Glacier, Cordillera Real, Bolivia, J. Geophys. Res., 104, doi:10.1029/1998JD200011, 1999.